sciendo

DOI: 10.2478/eces-2024-0018 ECOL CHEM ENG S. 2024;31(2):253-266

Sonia KOTOWICZ[1*], Mateusz KORZEC[1*], Maciej KAPKOWSKI[1]
and Agnieszka Katarzyna PAJĄK[2]

PHOTOPHYSICAL INVESTIGATIONS OF THE ORGANIC COMPOUNDS SYNTHESISED FROM WASTE POLY(ETHYLENE TEREPHTHALATE)

Abstract: This paper presents the photophysical investigations of two organic compounds synthesised directly by the aminolysis depolymerisation of the waste poly(ethylene terephthalate) (rPET) with aromatic amines, i.e., aniline and 3-amino-N-hexyl-1,8-naphthalimide without use of a catalyst. The chemical structure was confirmed by ^{1}H-NMR and ^{13}C-NMR, as well as FT-IR. The thermal, electrochemical and optical studies of the obtained derivatives were performed. The presented compounds were thermally stable up to 360 °C, and the glass transition temperature (T_g) occurred for the compound with the 1,8-naphthalimide units. The electrochemical investigations of the synthesised compounds have revealed one oxidation process and two reduction processes for the compound with the 1,8-naphthalimide fragments. The tested derivatives were characterised by a low-lying highest occupied molecular orbital (HOMO) level (below –6.09 eV) and an energy-band gap (E_g) below 3.10 eV. The obtained molecules were absorbed in the range of 204 nm - 445 nm and emitted light from a purple to a green spectral region deepened on the used solvent with low quantum yields. The blends with poly(3-hexylthiophene-2,5-diyl) (P3HT), which is used as a donor in the bulk heterojunction solar cells (BHJ), and amide derivative with 1,8-naphthalimide fragments were made, and the emission quenching of poly(3-hexylthiophene-2,5-diyl) (P3HT) was recorded. The presented results of the photophysical investigations have opened new possibilities for obtaining functional materials from recycled poly(ethylene terephthalate) (rPET).

Keywords: waste poly(ethylene terephthalate), recycling, synthesis, photophysical investigations

Introduction

Poly(ethylene terephthalate) (PET) belongs to the group of thermoplastic polymers and is widely used around the world. In addition to mechanical strength, PET has good chemical resistance to weak acids and alkali solutions, fats and oils [1-5]. The above properties allow PET to be used in the food packaging industry. Recycling of poly(ethylene terephthalate) can take place through physical, chemical (hydrolysis, alcoholysis, glycolysis, acidolysis, aminolysis), thermal processing or using the metabolism of microorganisms [6]. The physical recycling of the waste poly(ethylene terephthalate) involves its reuse by cleaning, grinding, melting and producing new elements (products) or

[1] University of Silesia, ul. Szkolna 9, 40-006 Katowice, Poland, phone +48 32 359 15 14, email: maciej.kapkowski@us.edu.pl, ORCID: SK 0000-0001-6021-0892, MK 0000-0002-8658-1031, MK 0000-0003-1425-4522
[2] Centre of Polymer and Carbon Materials, Polish Academy of Sciences, ul. M. Curie-Skłodowskiej 34, 41-819 Zabrze, Poland, phone +48 32 271 60 77 w. 114, email: apajak@cmpw-pan.pl, ORCID: 0000-0002-2684-4629
[*] Corresponding authors: sonia.kotowicz@us.edu.pl, mateusz.korzec@us.edu.pl

regranulating. Thermal decomposition of poly(ethylene terephthalate) can be carried out as a pyrolysis process (decomposition at high temperature in the presence of the inert gas) or gasification (transformation of PET into a gaseous and solid phase in the presence of air, oxygen, and water vapour or carbon dioxide) [7]. Biotechnological recycling (conducted using bacteria, fungi, marine microalgae or enzymes) involves biofragmentation of the polymer, its bio-assimilation and mineralisation [8]. The ester bond that connects the monomers in poly(ethylene terephthalate) can be hydrolysed by the hydrolytic enzymes (e.g. cutinase, lipase, esterase), leading to the recovery of ethylene glycol and terephthalic acid, which are the substrates of the PET polymerisation reaction [9]. In chemical methods, glycolysis is the primary method for chemical processing of PET, which uses glycol as a green solvent [10]. As a result of the chemical recycling reactions carried out in the disposal of PET, terephthalic acid is obtained, which, after purification, is used again in the reaction of obtaining poly(ethylene terephthalate) and obtaining polyester, polyamide fibers or foils. The second product of the reaction is ethylene glycol, which can be used to produce polyester resins, synthetic fibers, plasticisers and as a component of coolants due to its properties in the glycol-water mixture [11].

The problem with processing waste poly(ethylene terephthalate) is related to the diversity of the material received from the plastics recycling company. The variable content of plasticisers, fillers and other additives makes it much more challenging to adjust the thermal or chemical conditions during processing. Determining the complete chemical composition (organic and inorganic) is often impossible or economically unprofitable. Therefore, research is still being carried out to develop ecological, practical and economically profitable methods of recycling poly(ethylene terephthalate) (rPET).

In this publication, we present two amide derivatives (marked as PETA-1 and PETA-2) obtained in the one-pot reaction between recycled poly(ethylene terephthalate) (rPET) and the aromatic amines (aniline and 3-amino-N-hexyl-1,8-naphthalimide). PETA-1 (N,N'-diphenylterephthalamide) was synthesised by other research groups [12-14]. However, to the best of our knowledge, the recycled poly(ethylene terephthalate) was not used in N,N'-diphenylterephthalamide synthesis so far. Moreover, research on PETA-1 was focused on the biological activity and the crystallographic structure characterisation [13, 15, 16]. Therefore, in this work, we present for the first time synthesis from recycled PET and investigating the thermal, electrochemical and optical properties of the obtained products. The presented synthesis proposes recycling poly(ethylene terephthalate) into functional materials without additional purification or using catalysts as an eco-friendly synthesis. The presented results have opened new possibilities for the synthesis of the functional materials with the possibility of modifying their chemical structure.

Material and methods

The colourless poly(ethylene terephthalate) flakes from the waste bottle were purchased from Indorama Ventures PCL Bielsko-Biala (PVC (polyvinyl chloride) content 0.00 ppm - 50.00 ppm, PP/PE (polypropylene/polyethylene) content 0.00 ppm - 50.00 ppm, humidity 0.01 % - 1.2 %, dust content 0.01 % - 0.25 %, bulk density 240 kg/m^3 - 340 kg/m^3 (quality certificate no. 9950) and were grounded in a mill (Retsch SM100) obtained a fraction $\leq$ 1 mm. Aniline was purchased from Sigma Aldrich and purified by fractional distillation with zinc dust. 3-amino-N-hexyl-1,8-naphthalimide was obtained in a three-step synthesis starting from 3-nitro-1,8-naphthalic anhydride according to the recipe

described in the publication [17]. The nuclear magnetic resonance (^{1}H- and ^{13}C-NMR) spectra were recorded on a Bruker AC400 spectrometer in deuterated chloroform ($CDCl_3$) (PETA-2) and/or dimethyl sulfoxide-d6 (DMSO-d_6) (PETA-1) as solvent and tetramethylsilane (TMS) as the internal standard. Infrared spectra (FT-IR) were recorded on a Thermo Scientific Nicolet iS5 FT-IR Spectrometer in the range of 4000 cm^{-1} - 400 cm^{-1} as KBr pressed pellets (potassium bromide (KBr) before use was dried). PET used to NMR analysis was purchased from Sigma-Aldrich, CAS: 25038-59-9.

Synthesis of PETA-1 from the rPET

For a pressure reactor (ANTON PAAR 4760 with a 4838 controller and a 4760 heater) with a capacity of 300 cm^3, 16 g of crushed rPET (fraction ≤ 1 mm, without purification), 20 cm^3 of purified aniline and a magnetic dipole were introduced. The reaction was carried out at 180 °C for 20 hours, stirring at a speed of 350 rpm. After cooling the reactor, the obtained mixture was purified by washing with acetone (40 cm^3) to obtain 11 g of a white solid (reaction yield approximately 68.8 %) of PETA-1.

Analysis: $C_6H_4(CONHC_6H_5)_2$, 316.36 g/mol, ^{1}H-NMR (400 MHz, DMSO-d_6, δ, ppm): 10.40 (s, 2H), 8.10 (s, 4H), 7.79 (t, 4H, *J* = 7.9 Hz), 7.37 (d, 4H, *J* = 7.7 Hz), 7.13 (t, 2H, *J* = 7.2 Hz). ^{13}C-NMR (101 MHz, DMSO-d_6, δ, ppm): 165.22, 139.34, 137.83, 129.04, 128.16, 124.22, 120.84. FT-IR (KBr, υ, cm^{-1}): 3332 (N-H stretch), 3051 (C-H stretch aromatic), 1653 (C=O amide), 1529 (N-H).

Synthesis of PETA-2 from the rPET

For a pressure reactor (ANTON PAAR 4760 with a 4838 controller and a 4760 heater) with a capacity of 300 cm^3, 1 g of crushed rPET (fraction ≤ 1 mm, without purification), 3.23 g of N-hexylo-3-amino-1,8-naphthalimide and a magnetic dipole were introduced. The reaction was carried out at 180 °C for 20 hours, stirring at a speed of 350 rpm. After cooling the reactor, the obtained mixture was purified by washing with acetone (100 cm^3) to obtain 0.46 g of a light brown solid (reaction yield approximately 46.1 %) of PETA-2.

Analysis: $C_{44}H_{42}N_4O_6$, 722.83 g/mol, ^{1}H-NMR (400 MHz, $CDCl_3$, δ, ppm): 9.72 (d, 4H, *J* = 8.0 Hz), 9.29 (s, 2H), 8.83 (d, 4H, *J* = 7.3 Hz), 8.13 (t, 6H, *J* = 7.8 Hz), 4.33 - 4.20 (m, 4H), 1.82 - 1.75 (m, 4H), 1.54 - 1.31 (m, 12H), 1.91 (t, 6H, *J* = 6.8 Hz). ^{13}C-NMR (101 MHz, $CDCl_3$, δ, ppm): 163.59, 162.96, 143.42, 142.02, 133.76, 132.24, 130.75, 129.63, 129.15, 127.93, 126.78, 125.86, 125.25, 124.36, 123.25, 40.99, 31.56, 28.09, 26.83, 22.59, 14.06. FT-IR (KBr, υ, cm^{-1}): 3361 (N-H stretch), 3079 (C-H stretch aromatic), 2968, 2931 (aliphatic), 1708 (C=O imide ring), 1664 (C=O amide), 1623 (N-H).

The thermal behaviour was studied by thermogravimetric analysis (TGA) and differential scanning calorimetry (DSC). The heating rate was 10 °C/min for DSC measurements and 15 °C/min for TGA measurements under nitrogen atmosphere. DSC analysis were conducted on the TA DSC25 Discovery (TA instruments, accuracy 1 °C) and aluminum pots and TGA analysis on the PyrisTM1 TGA (Perkin Elmer, accuracy 1 °C) and platinum pots.

The electrochemical results were registered on Eco Chemie AutolabPGSTAT128n potentiostat using the glassy carbon electrode as the working electrode with 0.1 mol/dm^3 Bu_4NPF_6 (tetrabutylammonium hexafluorophosphate) electrolyte (Sigma-Aldrich) and dichloromethane (DCM, HPLC grade from Sigma-Aldrich) solution. The platinum coil and silver wire as the auxiliary and reference electrode were used, respectively. The moderate scan rate for the cyclic voltammetry and the differential pulse voltammetry was equal to 100 mV/s. The solutions were purged with argon before every measurement and performed

at 23 °C ±1 °C. The ferrocene couple (Fc/Fc^+) was used as the internal standard and the of Fc/Fc^+ was calculated to be equal to –5.1 eV as shown in the publication [18].

The UV-Vis absorption spectra were performed using the HITACHI U-2900 Spectrophotometer and 1 cm quartz cell for solutions. Photoluminescence spectra (PL) were performed using Varian Carry Eclipse Spectrometer and 1 cm quartz cell for solutions. The thin films were prepared by drop coating from a homogeneous chloroform solution (5 mg/cm^3). The blends were prepared by spin-coating (1000 rpm, 60 s; Laurell WS 650MZ-23NPPB) on the glass substrates from a homogeneous chloroform solution (5 mg/cm^3) with two weight ratios (1 : 1 as 50 wt.% : 50 wt.% and 4 : 6 as 40 wt.% : 60 wt.%). The thin films and blends were dried for 3 h in a vacuum oven (BUCHI Glass Oven B-585) at 50 °C. Solvents were purchased from Sigma-Aldrich with HPLC grade. The regioregular poly(3-hexylthiophene-2,5-diyl) (P3HT) was purchased from Ossila Ltd. The quantum yield (Φ_f) measurements in chloroform and dichloromethane were performed using the integrating sphere Avantes AvaSphere-80 (Edinburgh Instruments) and the absolute method.

Results and discussion

Characterisation of PETA-1 and PETA-2 synthesis products

The compounds marked as PETA-1 (N,N'-diphenylterephthalamide) and PETA-2 were obtained in the one-pot synthesis with waste poly(ethylene terephthalate) originating from the bottle (rPET) (cf. Fig. 1). The PETA-1 and PETA-2 structures are presented in Figure 1. The structures were confirmed by ^{1}H- and ^{13}C-NMR, HMQC (heteronuclear multiple quantum correlation) (for PETA-2) and FT-IR.

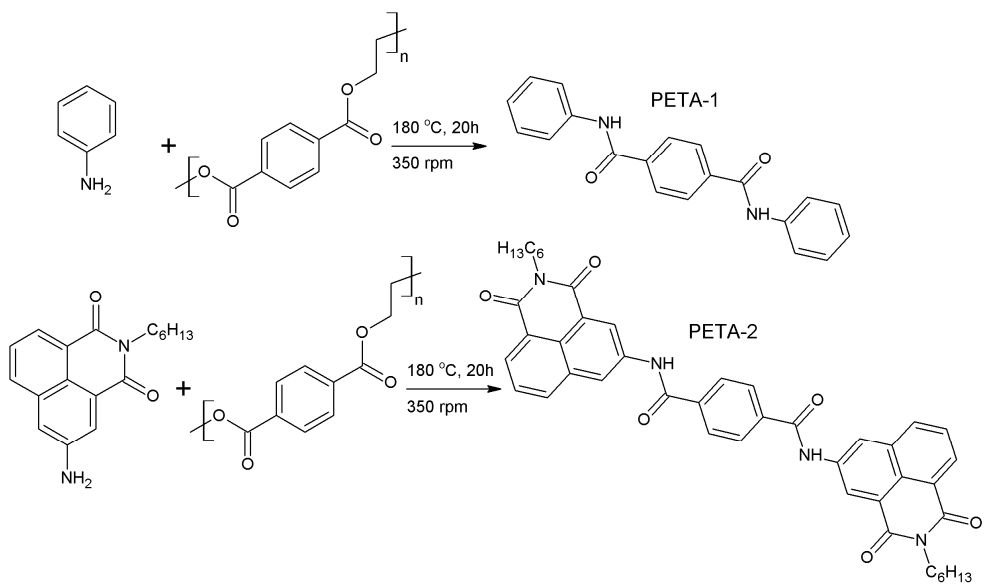


Fig. 1. The synthesis of PETA-1 and PETA-2 based on the direct aminolysis depolymerisation of the waste poly(ethylene terephthalate)

Figure 2 is shown superimposed ^{1}H-NMR spectra in the $CDCl_3$: TFA (4 : 1, v/v) arrangement for pure PET (Sigma Aldrich - pastille) and rPET (Indorama - ground petals). rPET was used in our syntheses. The addition of TFA in this mixture results in better solubility of PET samples, making the analysis of the content of this type of samples more accurate [19].

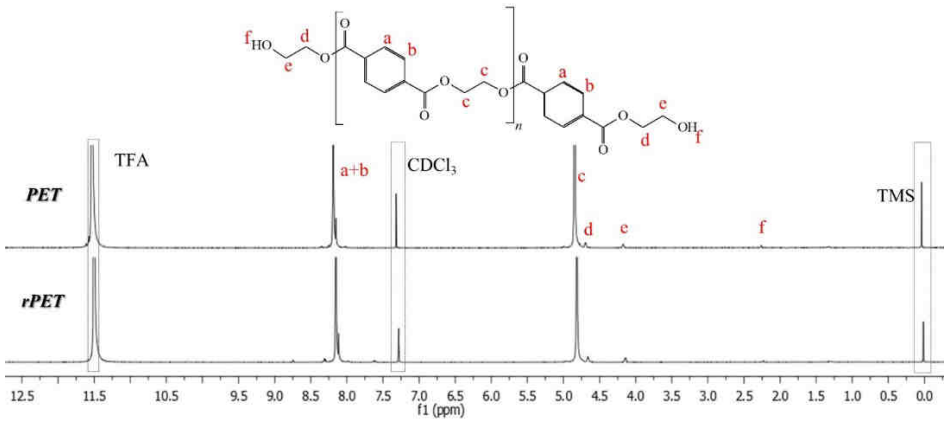


Fig. 2. ^{1}H-NMR of pure PET and rPET in $CDCl_3$: TFA (4 : 1, v/v)

The individual proton signals were assigned to a structure according to the designations (***a*** **-** ***f***). At a shift of approximately 8.14 ppm there is a signal characteristic of the protons of the aromatic ring (designation a + b). At a shift of 4.80 ppm there is a signal for aliphatic protons at the ester bond (designation c). The designations d, e and f refer to signals from protons for groups at the ends of PET. As can be seen, the NMR spectra for both samples are identical, with slight additional signals in the rPET sample at the 8.75 ppm or 7.60 ppm shift, which may be due to the additives used in the production of the PET bottles.

Figure 3 is shown the ^{1}H-NMR spectra of the substrates (aniline and 3-amino-N-hexylo-1,8-naphtalimide) and the obtained products prepared in DMSO-d_6 (PETA-1) and $CDCl_3$ (PETA-2).

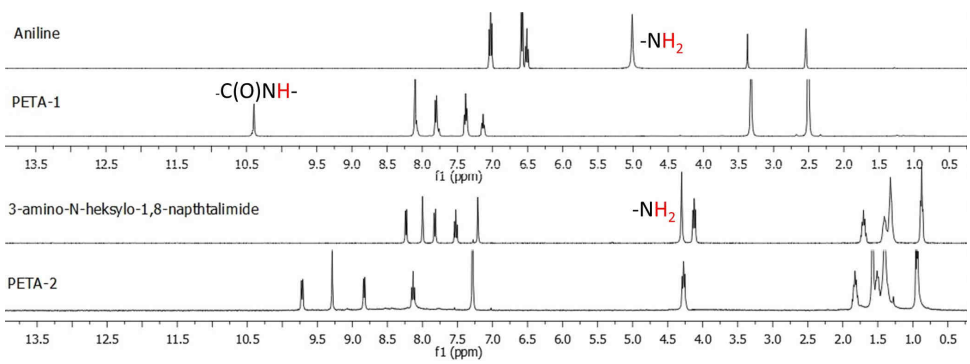


Fig. 3. Superimposed ^{1}H-NMR spectra of the corresponding amines (aniline and 3-amino-N-hexylo-1,8-naphthalimide) and the obtained products PETA-1 (in DMSO-d_6) and PETA-2 (in $CDCl_3$)

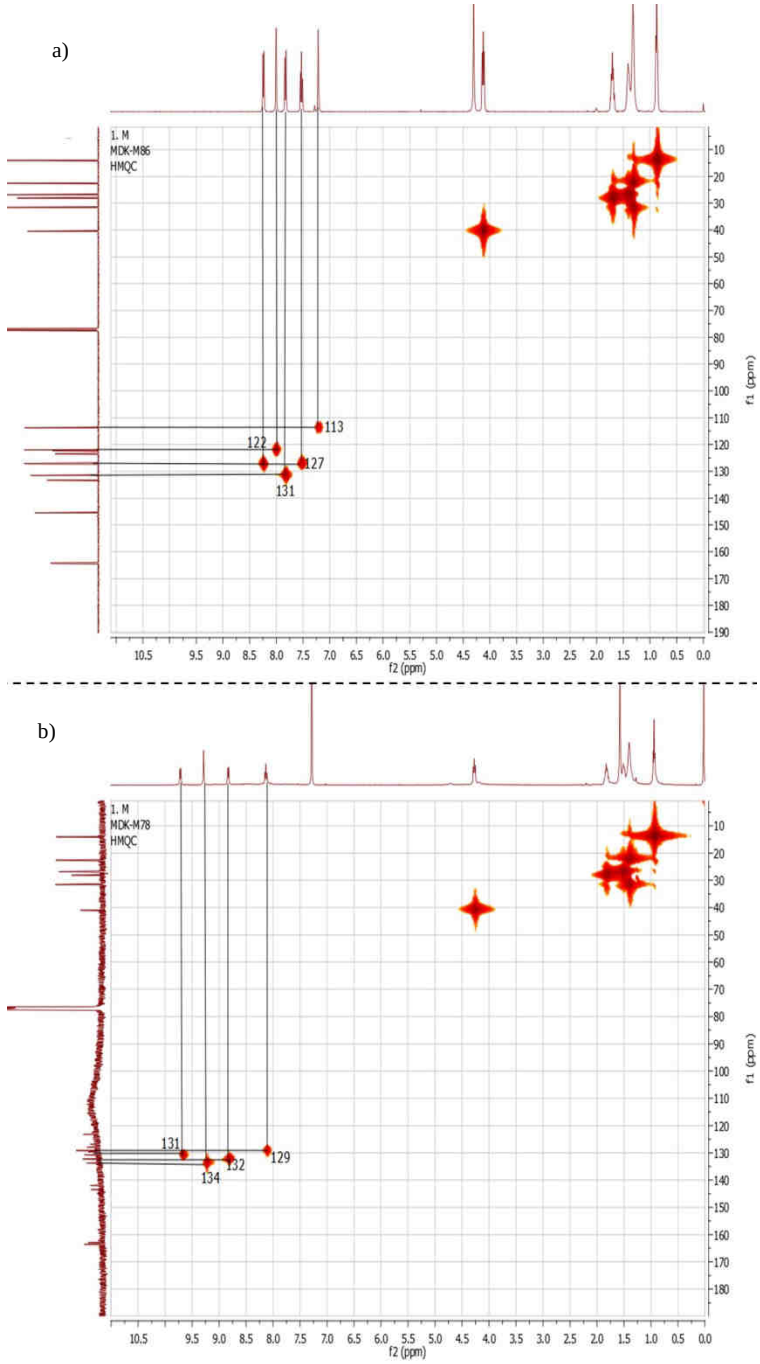


Fig. 4. HMQC spectra of: a) amine (3-amino-N-hexylo-1,8-napthalimide) and b) PETA-2 in $CDCl_3$

Regardless of the solvent used, an extension of the range of chemical shifts in the aromatic region can be observed, which is associated with the formation of a new amide bond. Moreover, there is a noticeable disappearance of the signal from the protons of -NH_2 group (4.90 ppm) and the appearance of the amide proton signal (10.40 ppm) in the case of the PETA-1 derivative performed in DMSO-d_6. Moreover, the characterisation for PETA-1 presented in this work is consistent with the description available in the literature [20]. However, in the case of PETA-2, in the ^{1}H-NMR spectra of the starting amine, the signal from the protons of the -NH_2 group occurs at a chemical shift of 4.30 ppm. In the product (PETA-2), the -NH_2 group is no longer visible (cf. Figs. 3 and 4), while signals from protons in the aromatic part increase the scope of the chemical shift. Interestingly, there is no visible signal from the -C(O)NH- group in this solvent ($CDCl_3$) and has also been reported in other publications [21]. In aromatic amides, the signals of aromatic protons may overlap with the proton from the amide or their delocalisation may occur, so the signal may not be clearly visible. Such considerations were carried out on a series of aromatic amides, showing the lack of signal for the amide proton on a spectrum taken in a pure solvent [22]. This effect may be related to the presence of the acceptor group in the attached naphthalimide.

The HMQC spectra for PETA-2 and the amine (cf. Fig. 4) for more detailed structural characterisation were performed. It can be noticed that all protons from the aromatic part appearing in the ^{1}H-NMR spectra are correlated with the appropriate carbon atoms. In amine, correlated carbon atoms occur in the range of 113 ppm - 131 ppm while in PETA-2 there is a visible change in this range - it narrows to 129 ppm - 134 ppm.

The FT-IR spectra is presented in Figure 5. The N-H stretching vibrations for PETA-1 was detected at 3332 cm^{-1} and for PETA-2 at 3361 cm^{-1}. The two signals of the aliphatic groups are visible at 2968 cm^{-1} and 2931 cm^{-1} in the case of PETA-2. The C=O amide absorption signals can be found at 1653 cm^{-1} (PETA-1) and 1664 cm^{-1} (PETA-2). The signal at 1708 cm^{-1} can be assigned to C=O imide ring vibrations visible in the PETA-2 chemical structure. The signals of the C=O, C-C-O and O-C-C stretching vibrations in the used for synthesis rPET were visible at 1718 cm^{-1}, 1249 cm^{-1} and 1094 cm^{-1}, respectively.

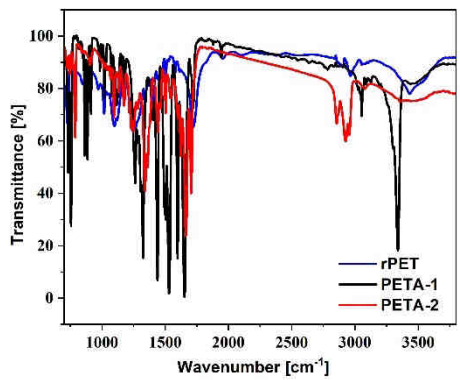


Fig. 5. FT-IR spectra of the PETA-1, PETA-2 and rPET

The thermal behaviour under heating was studied by thermogravimetric analysis (TGA) and differential scanning calorimetry (DSC) under nitrogen atmosphere. The results were collected in Table 1 and in Figure 6.

Table 1
The thermal stability (T_5) and the phase transition temperatures (T_{cc}, T_m) with the glass transition temperature (T_g) of the obtained amide derivatives

Mark	TGA		DSC			
			I heating scan	II heating scan		
	T_5	T_{max}	T_m	T_g	T_{cc}	T_m
	[°C]	[°C]	[°C]	[°C]	[°C]	[°C]
PETA-1	360	422	274,342	no	no	274,342
PETA-2	388	450	253	126	no	no
rPET	422 (401)[a]	464 (447)[a]	249	79	153	246

T_5 - the temperature of 5 % weight loss, T_{max} - the maximum decomposition rate read from the differential curve (DTG), T_m - melting temperature, T_{cc} - cold crystallisation temperature, T_g - glass transition temperature, no - not observed. DSC: 25 °C - 280 °C (PETA-1 to 350 °C). TG: 25 °C - 550 °C.
[a] - data for pure PET (Sigma Aldrich)

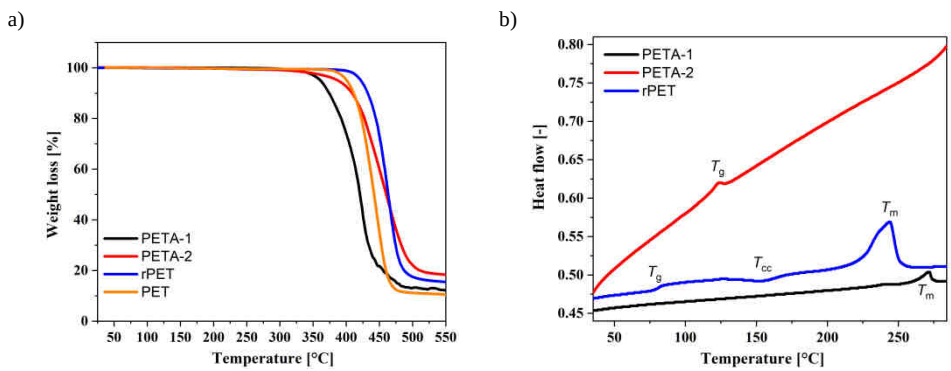


Fig. 6. a) TGA thermograms and b) DSC thermograms of the II heating scan of the obtained amide derivatives

Thermal properties of the poly(ethylene terephthalate) originating from the bottle (rPET) (fraction ≤ 1 mm, without purification) used for the synthesis was also tested. The crystalline nature of this polymer was reviled (the cold crystallisation temperature (T_{cc}) after the glass transition temperature (T_g) in the second heating scan). The 5 % weight loss (T_5) at the 401 °C was detected in the case of pure PET. The obtained temperature values are close to literature data for pure poly(ethylene terephthalate) [23].

The amide derivatives showed the T_5 at the temperature 360 °C for PETA-1 and 388 °C for PETA-2 and were characterised by a single-stage thermal decomposition (the one temperature of T_{max} (the maximum decomposition rate)). The amide derivatives in the first heating scan (DSC) were melted at 274 °C, 342 °C (PETA-1) and 253 °C (PETA-2), where the highest temperature was recorded for PETA-1. In the second heating scan, PETA-1 was melted at 274 °C and 342 °C (cf. Fig. 6b). Based on the literature, for PETA-1 the melting point were recorded between 333 °C - 346 °C [24]. The occurrence of the two melting temperature may indicate the existence of the two crystalline phases. The glass

transition temperature was recorded for PETA-2 (cf. Fig. 6a). This kind of behaviour is typical for molecular glasses when in the first heating scan the crystalline compound exhibited T_m, then the amorphous glass formed via a supercooled liquid, and in the second heating scan revealed the T_g. During further heating (after T_g), no phase transition temperatures for PETA-2 were detected. Based on the DSC analysis, PETA-1 and PETA-2 were obtained as the crystalline compounds, and PETA-2 can be transformed into molecular glass. The tested compounds are thermally stable, and the glass transition temperature at 126 °C allows their use as a material in optoelectronics.

Electrochemical and optical characterisation of PETA-1 and PETA-2

The electrochemical properties were investigated using two measurements method i) cyclic voltammetry (CV) and ii) differential pulse voltammetry (DPV). The results are gathered in Table 2 and the cyclic voltammograms are presented in Figure 7.

Table 2

Potentials of the oxidation and reduction processes (vs Fc/Fc^+) based on the electrochemical investigations

Mark	Method	E_{red}^1 [V]	$E_{red(onset)}^1$ [V]	E_{ox}^1 [V]	$E_{ox(onset)}^1$ [V]	E_{LUMO} [eV]	E_{HOMO} [eV]	E_g [eV]
PETA-1	DPV	–2.29	–2.18	1.28	0.99	–2.92	–6.09	3.17
	CV	–2.22[a]	–2.13	1.18[a]	1.06	–2.97	–6.16	3.19
PETA-2	DPV	–1.22	–1.10	1.30	1.11	–4.00	–6.21	2.21
	CV	–1.23[b]	–1.03	1.34[a]	1.17	–4.07	–6.27	2.20

$E_{HOMO} = (-5.1 - E_{ox(onset)})\cdot e^-$, $E_{LUMO} = (-5.1 - E_{red(onset)})\cdot e^-$, $E_g = E_{ox(onset)}^1 - E_{red(onset)}^1$. Solvent DCM and electrolyte 0.1 mol/dm^3 Bu_4NPF_6 (c = 10^{-3} mol/dm^3) and glassy carbon as a working electrode. [a] Irreversible process. [b] *Quasi*-reversible process. E_{ox} - the first oxidation process, E_{red} - the first reduction process, $E_{red(onset)}^1$ - the onset potential of the first reduction process, $E_{ox(onset)}^1$ - the onset potential of the first oxidation process. E_{HOMO} and E_{LUMO} as IP and EA

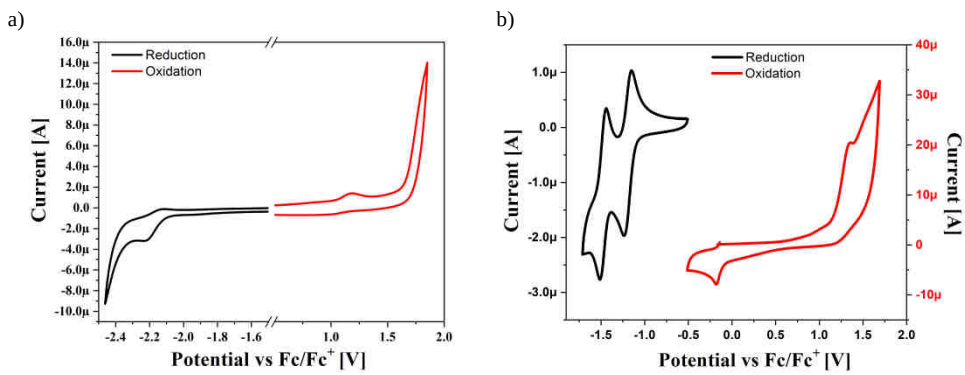


Fig. 7. The cyclic voltammograms of a) PETA-1 and b) PETA-2

PETA-1 was characterised with one reduction (E_{red}^1) and one oxidation (E_{ox}^1) processes and both processes were irreversible (ΔE > 150 mV). PETA-2, in the other hand, was characterised with two reductions and one oxidation processes. The reduction processes were *quasi*-reversible (150 mV > ΔE > 60 mV) and the oxidation process was irreversible. The reduction process was associated with the reduction of the electron-withdrawing fragments - the imide rings (C=O → C=O$^-$) in PETA-2. The two

reduction peaks were also seen in the symmetrical bis-(imino-1,8-naphthalimides) [25]. The differences in the position of the potentials may result from a different chemical environment, in the case of bis-imines due to the presence of the imine bonds, for PETA due to the presence of the amide bonds attached to the naphthalene ring.

Depending on the substituent attached via carbonyl carbon or -NH group, the amide bond can act as the electron-withdrawing or the electron-donor fragment. If an aromatic structure is attached via carbonyl carbon, it stabilises the resonance structure, and thus, the amide bond acts as an electron-withdrawing part of the molecule. However, if the aromatic ring is attached via -NH group, the imide bond acts as an electron-donor [26]. In our case, the aromatic ring is attached via carbonyl carbon and -NH group, allowing us to record the reduction and oxidation processes. In PETA-2 the reduction of imide rings was favourable, and the amide reduction was seen at –2.16 eV as an irreversible process.

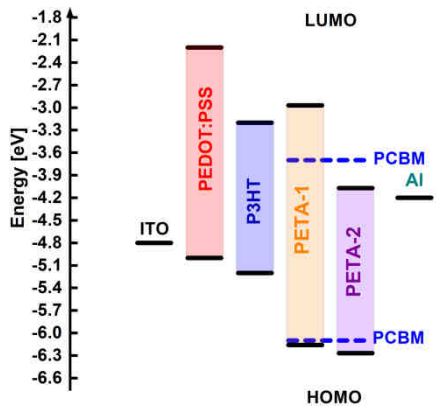


Fig. 8. The energy levels with the work function of the BHJ device components (the data taken from Ossila Ltd company and [25])

For good charge transportation and exciton diffusion, the base materials used in bulk heterojunction (BHJ) solar cells should have proper energy levels. The energy levels of the solar cell components should be matched to each other, and the electrodes should have appropriate work functions. Materials used in BHJ cells, such as PEDOT : PSS and P3HT, have appropriately adjusted HOMO levels to ITO electrode, and the PCBM ([6,6]-Phenyl-C61-butyric acid methyl ester) have appropriately adjusted LUMO (lowest unoccupied molecular orbital) level to Al electrode. Based on the HOMO and LUMO energy levels of the compound PETA-2, similar energy levels to PCBM was seen (cf. Fig. 8). Therefore, PETA-2 compound can be considered as an acceptor material.

The absorption (UV-Vis) and emission (PL) investigations were performed in the eleven solvents, and the solid state as the thin films on the glass substrate and blends with poly(3-hexylthiophene-2,5-diyl) (P3HT; in the case of PETA-2). The absorption and emission data from the solutions, thin films and blends are collected in Table 3 and Figure 9.

The UV-Vis and PL spectra in ethanol for the both compounds, toluene and acetone in the case of PETA-1 could not be recorded, which is a consequence of the lack of solubility. The absorption maxima (λ_{max}) at higher energies can be attributed to the electronic

transitions $\pi \rightarrow \pi^*$ in the aromatic ring (double bond system). PETA-1 was absorbed in the range characteristic for the aromatic rings (UV range, λ_{max} = 204 nm - 310 nm). PETA-2 was characterised by a complex subtle structure (several absorption maxima) in the UV-Vis range due to a more complex chemical structure than PETA-1. The λ_{max} approximately 340 nm can be attributed to $\pi \rightarrow \pi^*$ in the imide unit [17]. Moreover, the absorption maxima about 415 nm and 440 nm can be assigned to the naphthalene molecule part [27]. Based on the polarity of the solvents, slight changes to the λ_{max} positions were seen. The thin film from PETA-1 was obtained. However, the UV-Vis spectra were not recorded due to the permeability of the glass substrates (from 300 nm). PETA-2 in the form of the thin film was absorbed at 419 nm and 445 nm. The absorption spectra of the blends with P3HT revealed the λ_{max} at 425 nm and 445 nm as a shoulders and at about 516 nm, at 555 nm and about 600 nm as the characteristic λ_{max} of P3HT [28].

Table 3

The absorption and emission collected data based on the spectroscopic investigations

Mark	**Medium** ε[a]	λ_{max} **[nm]**	$\lambda_{em}(\Phi_f)$[b] **[nm] ([%])**	$\Delta\nu$[c] **[cm^{-1}]**
PETA-1	Hexane (1.88)	218	nr	-
	Toluene (2.38)	nr	nr	-
	Chloroform (4.8)	241, <u>283</u>	441(0.34)	12660
	THF (7.58)	240, 304	nr	-
	Dichloromethane (8.9)	231, <u>292</u>	439(0.26)	11468
	Acetone (20.7)	nr	nr	-
	Methanol (32.6)	204, 228, <u>282</u>	412	11189
	NMP (33)	308	361	4767
	DMF (37)	288	367	7474
	Acetonitrile (37.5)	232, <u>310</u>	432	9110
	DMA (37.8)	295	nr	-
	Thin film	nr	nr	-
PETA-2	Hexane (1.88)	275	434,465	13322
	Toluene (2.38)	319, 391[*], 415, <u>441</u>	451,474	503
	Chloroform (4.8)	316, 331[sh], 388, 413, <u>440</u>	447, 472(0.59), 504[sh]	356
	THF (7.58)	232, 312, 333[sh], 387, 413, <u>437</u>	441, 471	208
	Dichloromethane (8.9)	314, 331[*], 387, 412, <u>439</u>	446, 472(0.79), 501[sh]	358
	Acetone (20.7)	377[sh], 411, <u>436</u>	472, 498	1749
	Methanol (32.6)	<u>263</u>, 334[*], 435	442, 564	15398
	NMP (33)	335[sh], 380[*], 414, <u>442</u>	515	3207
	DMF (37)	308, 335[sh], 385[*], 413, <u>439</u>	518	3474
	Acetonitrile (37.5)	269, 331[sh], 376[sh], 410, <u>434</u>	442, 468, 501	417
	DMA (37.8)	335[sh], 384[*], 414, <u>440</u>	526	3716
	Thin film[d]	425, <u>452</u>	499[sh], 556[sh], 633	6574
	: P3HT 1:1	425[sh], 452[sh], 516[sh], <u>555</u>, 597[*]	604, 654[sh], 702[sh]	1462
	: P3HT 4:6	425[sh], 452[sh], 518[sh], <u>555</u>, 600[*]	622[sh], 651, 699[sh]	2657

[a] - dielectric constant, [b] - quantum yield, [c] - Stokes shifts calculated according to the equation $\Delta\nu = (1/\lambda_{max} - 1/\lambda_{em}) \cdot 10^7$ [cm^{-1}], [d] - Obtained from the chloroform solution, THF - tetrahydrofuran, NMP - N-methyloformamide, DMF - dimethyloformamide, DMA - dimethylacetamide, [sh] - shoulder, nr - not registered, [*] - taken from the second derivative. Underlined data indicates the excitation. $c = 10^{-5}$ mol/dm^3

The amide derivative PETA-1 was emitted light from a purple to a blue spectral region and PETA-2 from a blue to a green spectral region (cf. Table 3) in solutions. The presence of the 1,8-naphthalimide fragment in the molecule allowed the emission to be shifted to the lower energy [17, 25]. The emission of PETA-2 in the non-polar solvents was in the range

of 434 nm - 472 nm and the λ_{em} was shifted to the higher wavelengths in the polar solvents (498 nm - 564 nm). The compounds were characterised by a low quantum yields in chloroform and dichloromethane solutions (below 1 %). The emission in a red spectral region (λ_{em} = 633 nm) was recorded for the thin film of PETA-2.

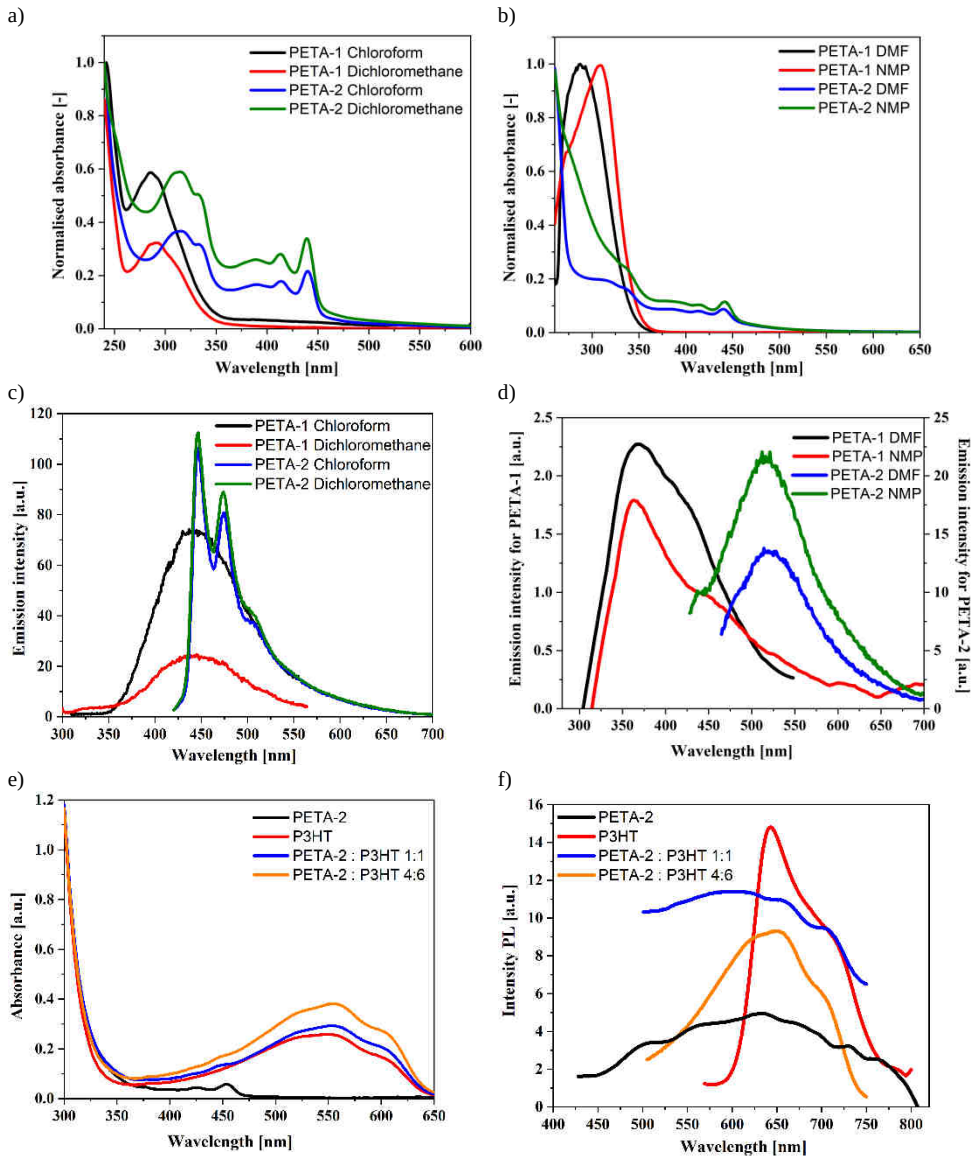


Fig. 9. The UV-Vis and PL spectra of PETA-1 and PETA-2 in selected a), c) non-polar, b), d) polar solvents (c = 10^{-5} mol/dm^3), and the UV-Vis e) and PL spectra f) of PETA-2 and blends with P3HT

Due to the low HOMO level of the PETA-2 compound (cf. electrochemical investigations) the blends with P3HT, which acts as a donor in BHJ solar cells (as already mentioned) were made. The compounds used as the active layers in the solar cells should have a broad absorption band and low emission intensity. P3HT (the donor molecule) has a broad absorption range but also emits light from 600 nm to 800 nm. In the construction of the BHJ solar cells active layer a mixture of a donor and an acceptor is used to quenching donor emission [28]. A quenching effect of the P3HT emission was noticed while the blends with PETA-2 were examined, which, in this case, is the desired effect. The emission quenching may suggest the effective transport and the separation of charges, which positively affects of the working BHJ solar cell [29].

Conclusion

The aminolysis depolymerisation of waste poly(ethylene terephthalate) was performed to obtain two amide derivatives. Based on the conducted research, it can be concluded that:

- depolymerisation aminolysis of poly(ethylene terephthalate) can occur without the use of catalysts and additional purification,
- obtained amide derivatives were thermally stable up to 360 °C and the appropriate selection of the amine in the PET depolymerisation reaction can lead to obtaining materials that can form molecular glasses,
- the acceptor nature (HOMO below –6.09 eV) of the amide derivative with the 1,8-naphthalimide groups was confirmed,
- synthesised compounds were absorbed in the range of 204 nm - 445 nm and emitted light from a purple to a green spectral region with the low quantum yields in solutions,
- the addition of the amide derivative can quench the P3HT emission used as a donor in the BHJ solar cells.

In the future, our research group have planned to test the PETA-2 compound in a mixture with P3HT as the active layer in the BHJ solar cell.

Acknowledgements

Research financed by the National Center for Research and Development (NCBR) under the grant: LIDER XI no. LIDER/39/0137/L-11/19/NCBR/2020.

References

[l] Nistico R. Polyethylene terephthalate (PET) in the packaging industry. Polymer Testing. 2020;90:106707. DOI: 10.1016/j.polymertesting.2020.106707.
[2] Chen S, Xie S, Guang S, Bao J, Zhang X, Chen W. Crystallization and thermal behaviors of poly(ethylene terephthalate)/bisphenols complexes through melt post-polycondensation. Polymers. 2020;12:3053. DOI: 10.3390/polym12123053.
[3] Suhaimi NAS, Muhamad F, Razak NAA, Zeimaran E. Recycling of polyethylene teraphthalate wastes: A review of technologies, routes, and applications. Polymer Eng Sci. 2022:1-21. DOI: 10.1002/pen.26017.
[4] Barber NA. Polyethylene Teraphthalate Uses, Properties and Degradation. New York: Nova Science Publishers, Inc; 2017. ISBN: 9781536119916.
[5] Qian K, Kumar A. Recent advances in utilization of biochar. Renew Sust Energy Rev. 2015;42:1055-64. DOI: 10.1016/j.rser.2014.10.074.
[6] Rabek JF. Polimery i ich zastosowanie interdyscyplinarne (Polymers and their interdisciplinary applications). Warszawa: Wydawnictwo Naukowe PWN; 2020. ISBN: 9788301210007.
[7] Saebea D, Ruengrit P, Arpornwichanop A, Patcharavorachot Y. Gasification of plastic waste for synthesis gas production. Energy Reports. 2020;6:202-07. DOI: 10.1016/j.egyr.2019.08.043.

[8] Soong YHV, Sobkowicz MJ, Xie D. Recent advances in biological recycling of polyethylene. Bioengineering. 2022;9:1-27. DOI: 10.3390/bioengineering9030098.
[9] Dissanayake L, Jayakody LN. Engineering microbes to bio-upcycle polyethylene terephthalate. Front Bioeng Biotechnol. 2021;2:656465. DOI: 10.3389/fbioe.2021.656465.
[10] Sabu T, Kanny K, Thomas MG, Rane A, Abitha VK. Recycling of Polyethylene Terephthalate Bottles. New York: Elsevier Inc; 2018. ISBN: 9780128113615. DOI: 10.1016/C2016-0-01084-7.
[11] Yue H, Zhao Y, Ma X, Gong J. Ethyleneglycol: properties, synthesis, and applications. Chem Soc Rev. 2012;41:4218-44. DOI: 10.1039/C2CS15359A.
[12] Larocca JP, Sharkawi MAY. Synthesis of some substituted amides of terephthalic and isophthalic acids. J Pharmaceutical Sci. 1967;56:916-8. DOI: 10.1002/jps.2600560732.
[13] Sellarajah S, Lekishvili T, Bowring C, Thompsett AR, Rudyk H, Birket ChR, et al. Synthesis of analogues of congo red and evaluation of their anti-prion activity. J Med Chem. 2004;47:5515-34. DOI:10.1021/jm049922t.
[14] Kurandina D, Huang B, Xu W, Hanikiel N, Daru A, Stroscio GD, et al. A porous crystalline nitrone-linked covalent organic framework. Communications. 2023;62:202307674. DOI: 10.1002/anie.202307674.
[15] Wang XL, Mu B, Lin HY, Yang S, Liu GCh. Two novel 3D copper(II) complex based on a rigid bis-pyridyl-bis-amide and two polycarboxylates mixed ligands: assembly, structures and properties. J Mol Structure. 2013;1036:380-5. DOI: 10.1016/j.molstruc.2012.12.001.
[16] Cheng H, Shang M, He Y, Shentu B, Gao Z. Synthesis and effect on N,N'-diphenylterephthalamide on crystallization of isotactic polypropylene. Polymer Sci. 2020;62:473-82. DOI: 10.1134/S1560090420050036.
[17] Kotowicz S, Korzec M, Siwy M, Golba S, Małecki JG, Janeczek H, et al. Novel 1,8-naphthalimides substituted at 3-C position: Synthesis and evaluation of thermal, electrochemical and luminescent properties. Dyes Pig. 2018;158:65-78. DOI: 10.1016/j.dyepig.2018.05.017.
[18] Bujak P, Kulszewicz-Bajer I, Zagorska M, Maurel V, Wielgus I, Proń A. Polymers for electronics and spintronics. Chem Soc Rev. 2013;42:8895-999. DOI: 10.1039/C3CS60257E.
[19] Pezz N, Janiska MCh, Imhof W. The first application of quantitative ^{1}H NMR spectroscopy as a simple and fast method of identification and quantification of microplastic particles (PE, PET and PS). Anal Bio Chem. 2018;411:823-33. DOI: 10.1007/s00216-018-1510-z.
[20] Dian HL, Meng FL, Yang ChX, Yan XP. Irreverible amide-linked covalent organic framework for selective and ultrafast gold recovery. Angew Chemie. 2020;59:17607-13. DOI: 10.1002/a.nie.202006535.
[21] Ackermann SM, Lachenmeier DW, Kuballa T, Schutz B, Spraul M, Bunzel M. NMR-based differentiation of conventionally from organically produced chicken eggs in Germany. Magn Reson Chem. 2019;57:579-88. DOI: 10.1002/mrc.3920143.
[22] Wilsens CHRM, Deshmukh YS, Noordover BAJ, Rastogi S. Influence of the 2,5-furandicarboxamide moiety on hydrogen bonding in aliphatic-aromatic poly(ester amide)s. Macromolecules. 2014;47:6196-206. DOI: 10.1021/ma501310f.
[23] Lima JC, Costa ARM, Sousa JC, Arruda SA, Almeida YMB. Thermal behavior of polyethylene terephthalate/organoclay nanocomposites: investigating copolymers as metrices. Polymer Composites. 2021;42:849-64. DOI: 10.1002/pc.25870.
[24] Cheng N, Yan Q, Liu S, Zhao D. Probing the intermolecular interactions of aromatic amides containing N-heterocycles and triptycene. CrystEngComm. 2014;16:4265-73. DOI: 10.1039/C4CE00089G.
[25] Kotowicz S, Korzec M, Pająk AK, Golba S, Małecki JG, Siwy M, et al. New acceptor-donor-acceptor systems based on bis-(imino-1,8-naphthalimide). Materials. 2021;14:2714-32. DOI: 10.3390/ma14112714.
[26] Espinoza EM, Clark JA, Derr JB, Bao D, Georgieva B, Quina FH, et al. How do amides affect the electronic properties of pyrene? ACS Omega. 2018;3:12857-67. DOI: 10.1021/acsomega.8b01581.
[27] Alonso-Navarro MJ, Harbuzaru A, Martinez-Fernandez M, Camero PP, Navarrere JTL, Ramos MM, et al. Synthesis and electronic properties of nitrogen-doped π-extended polycyclic aromatic dicarboximides with multiple redox processes. J Mater Chem C. 2021;9:7936-49. DOI: 10.1039/D1TC01239H.
[28] Amin MF, Gnida P, Kotowicz S, Małecki JG, Siwy M, Nitschke P, et al. Spectroscopic and physicochemical investigations of azomethines with triphenylamine core towards optoelectronics. Materials. 2022;15:7197-214. DOI: 10.3390/ma15207197.
[29] Kaim A, Piotrowski P, Zarębska K, Bogdanowicz KA, Przybył W, Kwak A, et al. Thermal imaging and deep optical and electrochemical study of C70 fullerene derivatives with thiophene, pyrrolidine or indene moieties along with electropolymerization with thiophene substituted imine: Blends with P3HT and PTB7. Electrochim Acta. 2022;426:140741. DOI: 10.1016/j.electacta.2022.140741.